

Progressive Token Length Scaling in Transformer Encoders for Efficient Universal Segmentation

Abhishek Aich[†], Yumin Suh[†], Samuel Schuster[†], Manmohan Chandraker^{†,‡}

[†]NEC Laboratories, America, USA, [‡]University of California, San Diego, USA

Abstract

A powerful architecture for universal segmentation relies on transformers that encode multi-scale image features and decode object queries into mask predictions. With efficiency being a high priority for scaling such models, we observed that the state-of-the-art method Mask2Former uses $>50\%$ of its compute *only* on the transformer encoder. This is due to the retention of a full-length token-level representation of all backbone feature scales at each encoder layer. With this observation, we propose a strategy termed **PRO**gressive Token Length **SCAL**ing for **E**fficient transformer encoders (PRO-SCALE) that can be plugged-in to the Mask2Former-style segmentation architectures to significantly reduce the computational cost. The underlying principle of PRO-SCALE is: progressively scale the length of the tokens with the layers of the encoder. This allows PRO-SCALE to reduce computations by a large margin with minimal sacrifice in performance ($\sim 52\%$ GFLOPs reduction with *no* drop in performance on COCO dataset). We validate our framework on multiple public benchmarks.

1 Introduction

The tasks of image segmentation (instance [1], semantic [2], and panoptic [3]) are recently being addressed together under the paradigm of “universal” image segmentation [4–9]. This is due to the evolution of transformer-based [10] approaches that can represent both *stuff* and *things* categories [3] using general tokens, leading to a diminished distinction among the tasks of semantic, instance, and panoptic segmentation. Success of the state-of-the-art universal segmentation framework Mask2Former (M2F) [5] can be attributed to its DETection TRansformer [11] or DETR-style architecture. This DETR-style segmentation (henceforth termed as M2F-style) framework exhibit exceptional performance across various segmentation tasks *without* the need for task-specific design choices, setting them apart from preceding modern panoptic segmentation frameworks [12–15].

The strong performance of M2F-style architecture, however, incurs significant computational overhead hindering their scalability. In this paper, we address this important problem of designing an efficient M2F-style architecture for universal segmentation model. In particular, we present **PRO**gressive Token Length **SCAL**ing for **E**fficient transformer encoders or PRO-SCALE that reduces the computational load occurring in the transformer encoder of such models with surprisingly low performance deterioration. M2F-style architectures contain a *backbone* (for multi-scale feature extraction from input images), a *transformer encoder* (to capture long-range dependencies and contextual relationships across the multi-scale backbone features), and a *transformer decoder* (for predicting the masks and labels) along with a segmentation module (see Fig. 1(a)). In efficient segmentation models, where the backbones are traditionally lightweight (SWIN-T [17] and Res50 [16]), cross-scale feature attention has been shown as a potent way to achieve high segmentation performance [5, 18]. However, it has been shown in [18–20] that due to a large number of query tokens introduced from multi-scale features of light backbones, the encoder incurs the *highest* computational cost. We make a similar observation in Fig. 1(b) for M2F where more than 50% of the compute comes from the encoder, given the standard backbones SWIN-T and Res50.

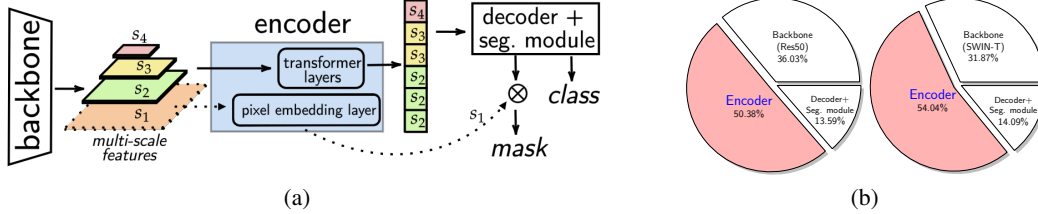


Figure 1: **Compute distribution.** (a) Mask2Former-style segmentation model (b) In the Mask2Former model using Res50 [16] and SWIN-T [17] backbones, the transformer encoder contributes the most to the overall computation cost, accounting for 54.04% and 50.38%, respectively.

Existing solutions [18, 19] for making DETR-style architectures efficient are *only* designed to handle *detection* tasks. For example, Lite-DETR [18] proposed to update larger and smaller scale features in different frequencies for efficient computation. RT-DETR [19] on the other hand, proposed a hybrid encoder that transforms multi-scale features into a sequence of image features through intra-scale interaction and cross-scale fusion. Such detection-based strategies do not suit the segmentation task: either they propose to discard the use of multi-scale features (as in [19]) or lack the ability to reduce computations induced due to constructing a pixel embedding map (as in [18]). This significantly reduces their impact on performance-efficiency trade-off for segmentation models (e.g. $\sim 33\%$ GFLOPs reduction but 11% segmentation accuracy drop).

To this end, we introduce PRO-SCALE, an efficient transformer encoder that has three key properties: (1) progressively increase the token length or input size at each encoder layer by introducing larger scale features in the deeper layers, (2) enhance small-scale features by explicitly modeling their inter-dependencies with the channels of higher scale features using a *Token Re-Calibration* (TRC) module, (3) simplifying the pixel embedding layer by replacing it with a *Light Pixel Embedding* (LPE) module. The fundamental idea of PRO-SCALE is to address the possible redundancy that arises from consistently maintaining a *full-length token sequence* across all layers in the encoder. For example as shown in Fig. 2(a), M2F uses tokens from multi-scale features across *all* encoder layers resulting in expensive computations. With PRO-SCALE’s progressively expanding tokens, the reduction in sequence length leads to significant FLOPs savings with minimal to negligible degradation in segmentation performance (see Fig. 2(b)). Extensive experiments show that PRO-SCALE based M2F-style architecture achieves a $\sim 52\%$ reduction in transformer encoder GFLOPs while maintaining the same segmentation performance. In particular, PRO-SCALE-M2F with SWIN-T backbone achieves a 52.82% PQ with 171.7 GFLOPs (vs. original performance of 52.03% PQ with 234.5 GFLOPs) on the COCO [21] dataset. To summarize, we make the following contributions:

- We present an efficient transformer encoder PRO-SCALE for M2F-style universal segmentation.
- PRO-SCALE operates on the fundamental idea of progressively expanding tokens along the encoder depth to address the computation redundancy. It is further assisted by a token re-calibration module and light pixel embedding module that effectively target performance improvement and computational reduction, respectively.
- Extensive experiments show that PRO-SCALE achieves the best performance-efficiency trade-off on two public benchmarks across diverse settings.

2 Related Works

DETR [11] embraces an end-to-end object detection approach with a set-prediction objective, discarding the need for manually crafted modules like anchor design and non-maximum suppression. Using the set prediction mechanism introduced in DETR, MaskFormer [4] proposed an approach that converts any existing per-pixel classification model into a mask classification model. This resulted in a universal segmentation architecture that demonstrated state-of-the-art performance across all segmentation tasks on public benchmarks in diverse settings [5, 8, 9, 22, 23] without task-specific design choices. In particular, it employs a transformer decoder to predict a set of pairs (a class prediction, a binary mask). Mask2Former [5] improved MaskFormer by using *masked* attention in the transformer decoder to restrict the attention to localized features centered around predicted seg-

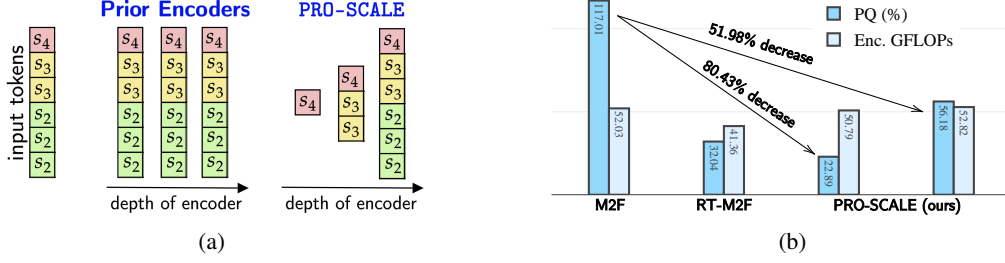


Figure 2: **Key idea and performance comparison of PRO-SCALE w.r.t. prior works.** (a) illustrates the key idea of PRO-SCALE to progressively extend the token length in the transformer encoder. $\{s_2, s_3, s_4\}$ represent different resolutions. In (b), we show two instantiations of our proposed transformer encoder PRO-SCALE, compared with Mask2Former (M2F) [5] and RT-M2F (an adaptation of [19]). PRO-SCALE eliminates 80.43% and 52% of encoder GFLOPs from M2F while maintaining the competitive performance. Results are computed on the COCO [21] dataset.

ments. Recently, [22] presented a DETR-style multi-task architecture by extending DINO [24] for both detection and segmentation tasks. PEM [8] introduced a MaskFormer based model that includes a multi-scale feature pyramid network to extract high-semantic-content features with context-based self-modulation to ensure efficiency. PRO-SCALE focuses on making Mask2Former-style universal segmentation models efficient.

In recent times, there have been some interesting efforts [8, 9, 15, 25–30] to make task-specific or *non-M2F-style* panoptic segmentation models efficient. For example, YOSO [13] introduced a lightweight panoptic segmentation model by utilizing a feature pyramid aggregator and separable dynamic decoders. ReMax [15] proposed a training pipeline to address the dominant impact of false positive mask assignments in panoptic segmentation by utilizing a separate semantic prediction head. Above methods contain specific model design choices or training strategies suited for the panoptic segmentation task. Unlike these, PRO-SCALE does not conform to one segmentation task and still shows competitive performances.

3 Methodology

Framework Overview. Following Mask2Former (M2F), PRO-SCALE is incorporated in a M2F-style framework. It is composed of a lightweight backbone, our novel transformer encoder design PRO-SCALE, and a transformer decoder with map and class prediction heads (each described next). The overall model framework is shown in Fig. 3. In particular, the input image is fed to the backbone to create multi-scale features. These features are flattened and updated by PRO-SCALE (introduced in Sec. 3.1) with gradual expansion of input tokens along with depth of intermediate encoder layers, allowing a better performance-efficiency trade-off. We further introduce a *Token Re-calibration* module (described in Sec. 3.1.1) within PRO-SCALE that enriches small-scale features with high-scale features to gain segmentation performance without significant computational overhead. The transformer decoder uses the representations from PRO-SCALE and learnable object queries to compute mask embeddings. Finally, a segmentation module uses the decoder output and per-pixel embeddings from PRO-SCALE for mask predictions. PRO-SCALE provides these per-pixel embeddings required for mask prediction using a parameter-free *Light-Pixel Embedding* module (described in Sec. 3.1.2). We start by introducing notations and model components, before diving into the details.

- A *backbone network* that extracts features from an input image $I \in \mathbb{R}^{H \times W \times 3}$. The backbone network can provide multi-scale feature maps $\{s_1, s_2, s_3, s_4\}$. The spatial resolutions are typically $1/4^2$, $1/8^2$, $1/16^2$, and $1/32^2$ of the input image, respectively. We will denote the token form of these features as s_1, s_2, s_3 , and s_4 , respectively.
- A *Transformer encoder*, that enhances the image features $\{s_2, s_3, s_4\}$ for the transformer decoder and creates a per-pixel embedding map from s_1 for the final segmentation module. Feature enhancement is performed on a token representation $P \in \mathbb{R}^{K \times C}$, where $K = \sum (HW/32^2 +$

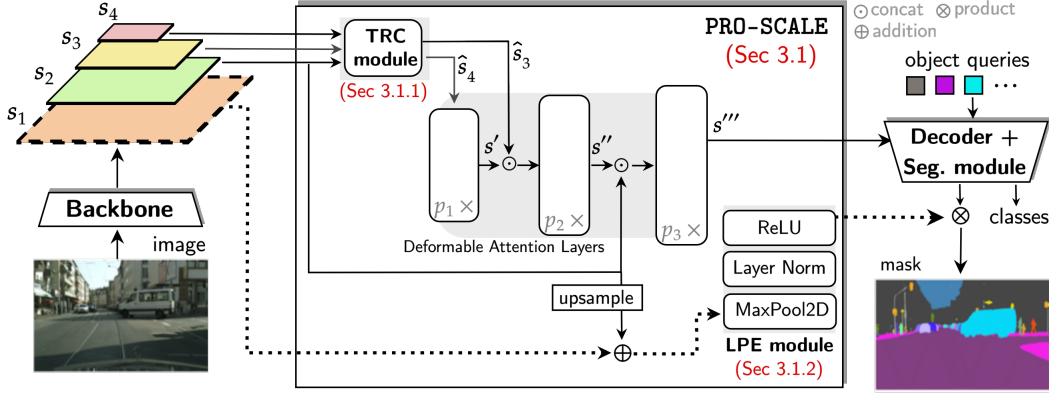


Figure 3: **Proposed framework.** Our model includes our transformer encoder PRO-SCALE (Sec. 3.1), designed to reduce the computational load. $\{s_i\}$ s represent the multi-scale backbone features. PRO-SCALE uses a *Token Re-Calibration* (TRC) module (Sec. 3.1.1) to enhance s_4 and s_3 using s_2 and outputs \hat{s}_4 and \hat{s}_3 , respectively. Further, s_1 goes through our efficient *Light-Pixel Embedding* (LPE) module (Sec. 3.1.2) to create pixel embeddings for mask prediction. p_1 , p_2 and p_3 represent encoder layer frequency. $\{s', s'', s'''\}$ represent the outputs of respective layers.

$HW/16^2 + HW/s^2$) and $C = 256$ [5]. This P is composed of concatenated $\{s_2, s_3, s_4\}$ obtained via flattening the spatial dimensions. The transformer encoder usually consists of several stacked transformer blocks. Following M2F, our framework also consists of six deformable attention transformer [31] layers that includes a self-attention block and a feed-forward block.

- A *Transformer decoder along with segmentation module* that decodes binary masks from the modulated image features using a set of randomly initialized object queries. The transformer decoder consists of three stages, with each stage consisting of three transformer layers [10]. Each layer includes a self-attention block, a cross-attention block, and a feed-forward block. Each layer only handles tokens of one scale of features for efficiency [5].

As described above, the original transformer encoder results in significantly expensive computations as it maintains the complete token length of P for all layers. Simply dropping larger scale features results in poor localization, especially in small objects [18]. For example, removing features s_1 and s_2 results in a degradation of $\sim 5\%$ AP compared to original model. Moreover, large-scale features are required to produce pixel embedding maps for strong segmentation performance. We will now explain how our approach tackles these obstacles.

3.1 PRO-SCALE: Proposed Transformer Encoder

Intuition. The bottleneck towards an efficient encoder are excessive large-scale features, where most of which are not informative but contain local details for different objects [18]. In order to better handle their usage in the encoder, we can leverage the composition of multi-scale features from the backbone: (1) The limited quantity of small-scale features (e.g. s_3, s_4) captures abundant semantics. (2) The larger quantity of large-scale features (e.g. s_1, s_2) captures crucial local features important for segmenting varying scale of objects. For example, assuming a SWIN-T backbone based M2F, $\{s_2, s_3, s_4\}$ result in $\{76.19\%, 19.04\%, 4.76\%\}$ token contributions, respectively. Therefore, we propose to prioritize enrichment of tokens from small scale features earlier than the large scale features.

Encoder structure. We build upon deformable attention as it exhibits linear complexity with the number of feature queries (in our case, represented by P). We create three splits of P (following the three scales):

$$P_1 = \mathcal{C}(s_4) \in \mathbb{R}^{K_1 \times C}, \quad (1)$$

$$P_2 = \mathcal{C}(s', s_3) \in \mathbb{R}^{K_2 \times C} \quad (2)$$

$$P_3 = \mathcal{C}(s'', s_2) \in \mathbb{R}^{K_3 \times C} \quad (3)$$

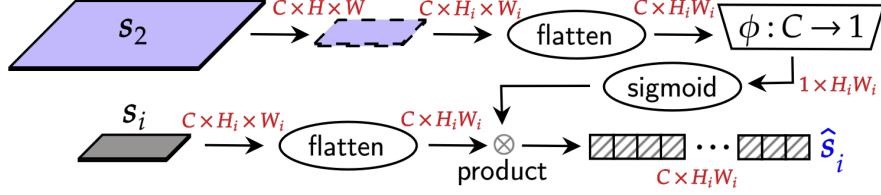


Figure 4: **Token Re-Calibration (TRC) module.** This unit first interpolates s_2 to the size of the target smaller-scale feature s_i . Then, the spatially flattened and resized s_2 is passed through a channel reduction layer ϕ (followed by sigmoid function) to produce an attention map. This map is imposed on the spatially flattened s_i to create \hat{s}_i .

Here, $\mathcal{C}(\cdot)$ denotes the concatenation operation along the token size dimension, $K_3 = \sum(HW/32^2 + HW/16^2 + HW/8^2)$, $K_2 = \sum(HW/32^2 + HW/16^2)$, and $K_1 = HW/32^2$. These splits are then fed to three stages of the deformable attention transformer layers sequentially. The output of these stages are s' , s'' , and s''' , respectively. s''' is subsequently fed to the decoder. Each stage is repeated p_1 , p_2 and p_3 times before propagating the tokens to the next stage. This results in updation of s_4 for $(p_1 + p_2 + p_3)$, s_3 for $(p_2 + p_3)$, and s_2 for p_1 times, gradually *expanding* the token length of inputs to intermediate layers in PRO-SCALE. As we show in Sec. 4, this strategy reduces computing load by significant margins while maintaining performance.

3.1.1 Token Re-Calibration (TRC) Module

Intuition. Skipping the propagation of s_2 in the initial layers may lead to errors in predicted panoptic maps due to missing information from this feature scale. To avoid such map errors caused by imperfect token representations, we propose to calibrate the s_3 and s_4 using s_2 in our TRC module. This module aims to enhance small-scale features $s_i \in \{s_3, s_4\}$ using large-scale feature s_2 without increasing the computations in PRO-SCALE transformer layers.

TRC structure. To utilize strengths of s_2 in smaller scales, we employ contrastive attention. In particular, we propose to enrich the tokens of s_i by projecting s_2 on s_i via an attention map. This attention map is obtained by using a channel reduction layer ϕ followed by a sigmoid function. As illustrated in Fig. 4, the final tokens \hat{s}_i are obtained as (\otimes represents elementwise multiplication):

$$\hat{s}_i = s_i \otimes \text{sigmoid}(\epsilon \phi(s_2)) \quad (4)$$

With above, Eq. 2, 3 translate to $P_1 = \mathcal{C}(\hat{s}_4)$ and $P_2 = \mathcal{C}(s', \hat{s}_3)$. We choose $\phi(\cdot)$ to be a linear layer and set temperature $\epsilon = 0.1$, keeping computations negligible.

3.1.2 Light-Pixel Embedding (LPE) Module

Intuition. Strong performance of M2F depends on multi-scale features computed from the backbone [5]. Tokens $\{s_2, s_3, s_4\}$ are fed to the encoder layers to compute s''' in order to produce per-segment embeddings in the transformer decoder. s_1 , on the other hand, serves the purpose of creating the per-pixel embedding map \mathcal{E}_{emb} . However, it results in high computational load due to use of convolutional layer in original M2F. Hence rather than dropping s_1 , we assess the existing learnable module with a simpler module in our design.

LPE structure. We propose to use a simple maxpooling layer followed by normalization and non-linearity to compute \mathcal{E}_{emb} . The goal of our LPE module is to mitigate this overhead while keeping the advantages of s_1 in producing \mathcal{E}_{emb} . We observe it reduces almost $\sim 45\%$ GFLOPs in the encoder architecture, but doesn't significantly harm the overall model's segmentation performance. In our implementation, we use a pooling kernel size of 3.

4 Experiments

In this section, we evaluate PRO-SCALE based M2F architecture on two benchmarks on all segmentation tasks. *First*, we observe that PRO-SCALE is extremely effective in reducing computational load while providing best trade-offs compared to baselines (Tab. 1, 2). *Second*, we analyze each

Table 1: **COCO evaluation.** PRO-SCALE is extremely competitive against the baselines on COCO with at least 51.99% GFLOPs reduction compared to M2F with no performance drop. Non-M2F-style architectures are colored in gray.

Model	Performance (\uparrow)			GFLOPs (\downarrow), (% decrement)	
	PQ	mIOU _p	AP _p	Total	Tx. Enc.
Backbone: SWIN-T					
M2F [5]	52.03	62.49	42.17	234.50	117.00
Lite-M2F [18]	52.70	63.08	41.10	188.00 (-19.83)	79.78 (-31.81)
RT-M2F [19]	41.36	61.54	24.68	158.30 (-32.49)	59.66 (-49.01)
PRO-SCALE (1, 1, 1)	50.79	62.39	39.57	137.10 (-41.54)	22.89 (-80.44)
PRO-SCALE (2, 2, 2)	52.12	63.21	41.58	154.40 (-34.16)	39.53 (-66.21)
PRO-SCALE (3, 3, 3)	52.82	63.49	42.60	171.70 (-26.78)	56.18 (-51.99)
Backbone: Res50					
M2F [5]	51.73	61.94	41.72	229.10	135.00
MF [4]	46.50	57.80	33.00	181.00 (-20.99)	– (–)
PEM [8]	46.38	55.95	34.25	110.90 (-51.59)	– (–)
YOSO [13]	48.40	58.74	36.87	114.50 (-50.02)	– (–)
RAP-SAM [30]	46.90	–	–	123.00 (-46.31)	– (–)
ReMax [15]	53.50	–	–	– (–)	– (–)
PRO-SCALE (1, 1, 1)	50.31	60.66	39.56	131.40 (-42.65)	30.25 (-77.59)
PRO-SCALE (2, 2, 2)	51.21	61.53	40.66	148.8 (-35.05)	48.85 (-63.48)
PRO-SCALE (3, 3, 3)	51.45	61.58	41.45	166.1 (-27.50)	67.45 (-50.03)

additional component of PRO-SCALE (TRC and LPE units) in Tab. 3, 5, and 7, and Fig. 5. *Third*, we analyze the impact of different backbones and their pre-training strategies in Tab. 6 and Fig. 8. Finally, we visualize some segmentation examples in Fig. 9. In our Supplementary material, we provide our training, dataset (for COCO [21] and Cityscapes [32]), and baseline details. We also provide additional results on larger backbones, analysis with object detection as well as open-vocab segmentation which further underscore the strengths of our encoder. For brevity, we will denote our overall framework as PRO-SCALE.

Evaluation metrics. We evaluate PRO-SCALE and baselines in the *universal* segmentation setting. This means, following [5], PRO-SCALE’s evaluation is performed using a model trained *exclusively* with panoptic segmentation annotations. For panoptic segmentation, the conventional PQ (Panoptic Quality [3]) metric is used. Following [5], we report AP_p (Average-Precision [21]) metric for instance segmentation. This is computed on the ‘thing’ categories from the instance segmentation annotations. For semantic segmentation, we report mIOU_p (mean Intersection-over-Union [33]) by merging instance masks from the same category. Here, subscript *p* denotes evaluation after training with panoptic segmentation annotations. For computing the GFLOPs, we use image scale of (800, 1333) for COCO dataset, and (1024, 2048) for Cityscapes dataset. All models are trained and evaluated on the *train* and *validation* split, respectively.

Architecture Details. We focus on standard lightweight backbones Res50 [16], SWIN-Tiny [17], and MViT2-Tiny [34], pre-trained on ImageNet-1K [35]. We use PRO-SCALE as the transformer encoder. As per Sec. 3, we use different integer values of (*p*₁, *p*₂, *p*₃) to instantiate different depths of the stages in PRO-SCALE. We directly adopt the M2F’s decoder that consists of masked attention [5] with 9 layers in total and 100 learnable queries. Similar to M2F’s round robin design, PRO-SCALE feeds {*s*₂, *s*₃, *s*₄} into successive transformer decoder layers.

4.1 Main Results

The analysis on the COCO dataset is presented in Tab. 1. We use M2F [5] as reference for performance and present the following insights. *First*, PRO-SCALE is significantly computationally cheaper than baseline efficient M2F-style models such as Lite-M2F and RT-M2F. For example with SWIN-T backbone, PRO-SCALE achieves a PQ of 52.82 and with a computational cost of 171.70 GFLOPs. This PQ is 11.46 points better than that of RT-M2F, while enabling a $\sim 52\%$ lighter transformer encoder. Compared to Lite-M2F, PRO-SCALE shows a better overall segmentation while decreasing approximately $\sim 52\%$ of GFLOPs compared to $\sim 32\%$ of Lite-M2F. Similar performance improve-

Table 2: **Cityscapes evaluation.** PRO-SCALE shows strong efficiency trade-off compared to the baselines on Cityscapes, *e.g.* 51.96% (SWIN-T) and 50.17% (Res50) GFLOPs reduction and little-to-no accuracy drop. Non-M2F-style models are colored in gray. † trained for 200K iterations.

Model	Performance (\uparrow)			GFLOPs (\downarrow), (% decrement)	
	PQ	IoU _p	AP _p	Total	Tx. Enc.
Backbone: SWIN-T					
M2F [5]	64.00	80.77	39.26	537.8	281.00
Lite-M2F [18]	62.29	79.43	36.57	428.7 (-20.29)	172.00 (-38.79)
RT-M2F [19]	59.73	77.89	31.35	361.1 (-32.86)	130.00 (-53.74)
PRO-SCALE (1, 1, 1)	60.58	78.29	32.97	311.9 (-42.00)	055.14 (-80.38)
PRO-SCALE (2, 2, 2)	62.37	78.62	35.97	352.0 (-34.55)	095.24 (-66.11)
PRO-SCALE (3, 3, 3)	63.06	77.94	37.81	392.1 (-27.09)	135.00 (-51.96)
Backbone: Res50					
M2F [5]	61.86	76.94	37.35	524.1	291.0
PEM [8]	61.10	—	—	236.6 (-51.59)	— (-)
YOSO [13]	59.70	76.05	33.76	265.1 (-49.42)	— (-)
ReMax [†] [15]	65.40	—	—	294.7 (-43.77)	— (-)
PRO-SCALE (1, 1, 1)	59.70	77.19	32.77	298.1 (-43.12)	65.21 (-77.59)
PRO-SCALE (2, 2, 2)	60.89	76.61	34.95	338.2 (-35.47)	105.0 (-63.92)
PRO-SCALE (3, 3, 3)	61.87	78.44	37.33	378.3 (-27.82)	145.0 (-50.17)

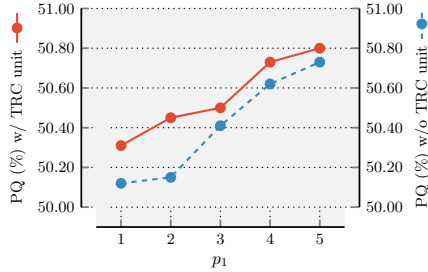


Table 3: **Impact of TRC module.** Use of s_2 via TRC to enhance $\{s_3, s_4\}$ improves the overall performance with light computational load. Here, backbone = Res50, dataset = COCO.

Table 4: **Impact of ϵ on TRC.** Temperature scaling ϵ of 0.1 shows the best performance. Here, backbone = SWIN-T, dataset = Cityscapes.

ϵ	PQ(%)
0.01	60.05
0.10	60.58
1.00	60.32
5.00	60.41
10.00	60.34

ments can be observed over M2F and MaskFormer [4] with Res50 backbone. *Second*, PRO-SCALE outperforms non-M2F-style models YOSO [13] in panoptic segmentation by at least ~ 2 points. YOSO has a slightly better computational load than PRO-SCALE, while ReMax [15] has competitive accuracy. Note that, ReMax focuses on the training pipeline of panoptic segmentation [15], which is orthogonal to our approach to design efficient segmentation architectures. Similarly, in comparison with a recent universal segmentation architecture PEM [8] with Res50 backbone, PRO-SCALE shows stronger results in severe GFLOPs reduction settings ($p_1, p_2, p_3 = 1, 1, 1$). The analysis on Cityscapes dataset segmentation is shown in Tab. 2. Similar to COCO, PRO-SCALE is computationally most efficient compared to both M2F-style models (Lite-M2F and RT-M2F) and at-par with non-M2F-style models (YOSO and ReMax [15]) with extremely competitive performance. For example, PRO-SCALE with SWIN-T backbone achieves 63.06 PQ vs. Lite-M2F’s 62.29 PQ while having comparatively $\sim 27\%$ less GLOPs than M2F. Similarly, compared to non-M2F-style models in Res50 backbone, PRO-SCALE demonstrates competitive performance with *no specific* panoptic segmentation design like YOSO [13], or much fewer training iterations with specific panoptic segmentation training strategies like ReMax [15] (200K vs 90K iterations).

4.2 Ablation Study

Impact of TRC module. Our TRC module is designed to incorporate the benefits of large scale feature s_2 without increasing computational overhead in PRO-SCALE. In Tab. 3, we can see that the TRC module consistently improves the performance of the proposed framework demonstrating the

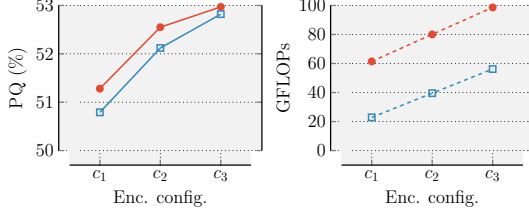


Figure 5: **Impact of LPE module.** Per-pixel embeddings produced by LPE do not significantly harm the performance but demonstrate a strong impact on the computational reduction. Here, backbone= SWIN-T, PRO-SCALE configuration: $c_1 = (1, 1, 1)$, $c_2 = (2, 2, 2)$, $c_3 = (3, 3, 3)$, models = w/o LPE and w/ LPE, dataset = COCO.

Figure 6: **Impact of different backbones.** PRO-SCALE can provide significant efficiency boosts across various backbones. Here, $(p_1, p_2, p_3) = (1, 1, 3)$, dataset = COCO.

Backbone type	Performance (\uparrow)			GFLOPs (\downarrow), (% decrement)	
	PQ	mIOU _p	AP _p	Total	Tx. Enc.
SWIN-T	52.03	62.49	42.17	234.5	117.00
	52.40	62.66	41.62	164.7 (-29.77)	54.77 (-53.19)
Res50	51.73	61.94	41.72	229.1	135.00
	51.35	61.53	40.82	158.6 (-30.77)	59.44 (-55.97)
MViT-T	54.11	64.39	44.54	244.6	130.00
	53.70	64.17	43.53	174.1 (-28.82)	54.77 (-57.87)

Table 5: **LPE module with Lite-M2F.** LPE can be flexibly integrated to improve the computational load of Lite-M2F [18] with minimal performance degradation. Backbone = SWIN-T.

Dataset	Model	Performance			GFLOPs (% decrement)	
		PQ	mIOU _p	AP _p	Total	Tx. Enc.
COCO	Lite-M2F	52.70	63.52	42.26	188.00	79.78
	+ LPE	52.32	63.08	41.10	154.60 (-17.77)	43.92 (-44.95)
Cityscapes	Lite-M2F	62.29	79.43	36.57	428.7	172.00
	+ LPE	61.35	79.05	35.91	351.4 (-18.03)	94.69 (-44.95)

Figure 7: **Analysis of PRO-SCALE configurations** (p_1, p_2, p_3) . Increments in different p_i shows different performance-computational trade-off. Backbone = SWIN-T.

p_1, p_2, p_3	Performance (\uparrow)			GFLOPs (\downarrow), (% decrement)	
	PQ	mIOU _p	AP _p	Total	Tx. Enc.
Dataset: Cityscapes					
original	64.00	80.77	39.26	537.8	281.00
(1, 1, 1)	60.58	78.29	32.97	311.9 (-42.00)	055.14 (-80.38)
(3, 1, 1)	61.38	78.58	33.75	314.7 (-41.48)	057.93 (-79.38)
(1, 3, 1)	61.63	78.67	35.26	326.3 (-39.33)	069.62 (-75.22)
(1, 1, 3)	62.32	79.49	36.97	374.8 (-30.31)	118.00 (-58.01)
Dataset: COCO					
original	52.03	62.49	42.17	234.50	117.00
(1, 1, 1)	50.79	62.39	39.57	137.1 (-41.54)	22.89 (-80.44)
(3, 1, 1)	51.69	62.81	40.46	138.7 (-40.85)	26.87 (-77.03)
(1, 3, 1)	51.76	63.23	41.07	143.8 (-38.68)	32.29 (-72.40)
(1, 1, 3)	52.40	62.66	41.62	164.7 (-29.77)	54.77 (-53.19)

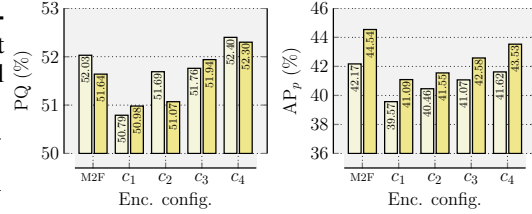


Figure 8: **Impact of pre-trained weights.** PRO-SCALE provides significant computational boosts, irrespective of backbone pre-trained weights. Here, backbone/dataset= SWIN-T/COCO, weights = supervised/ MoBY [36] on IN1K [37], PRO-SCALE config.: $c_1 = (1, 1, 1)$, $c_2 = (3, 1, 1)$, $c_3 = (1, 3, 1)$, $c_4 = (1, 1, 3)$.

efficacy of this unit. Moreover, this unit only costs 0.006 GFLOPs for the COCO dataset. Finally, we also analyze the impact of ϵ on the TRC module in Tab. 4 and find that it overall improves the performance of segmentation with best performance at $\epsilon = 0.1$.

Impact of LPE module. Our LPE module is aimed to drastically decrease the computational overhead without impairing the segmentation performance in PRO-SCALE. To analyze this, we compare LPE with the M2F’s convolutional layer based embedding layer module in Fig. 5. Here, we can observe that compared to this convolutional unit with learnable parameters, LPE is extremely effective. For example, for PRO-SCALE configuration $c_3 = (3, 3, 3)$, LPE reduces the computations by $\sim 40\%$ with performance degradation of 0.12 PQ points. Similarly, $c_2 = (1, 1, 1)$ and $c_2 = (2, 2, 2)$ provide similar computational benefits with 0.43 PQ points degradation. This demonstrates the favorable performance-computation trade-off LPE provides in PRO-SCALE. To further demonstrate the potency of our proposed LPE module, we incorporate LPE in Lite-M2F and analyze the results in Tab. 5. We can observe that LPE shows similar impact on Lite-M2F: $\sim 45\%$ less transformer encoder GLOPS with only ~ 0.5 -1 PQ point trade-off.

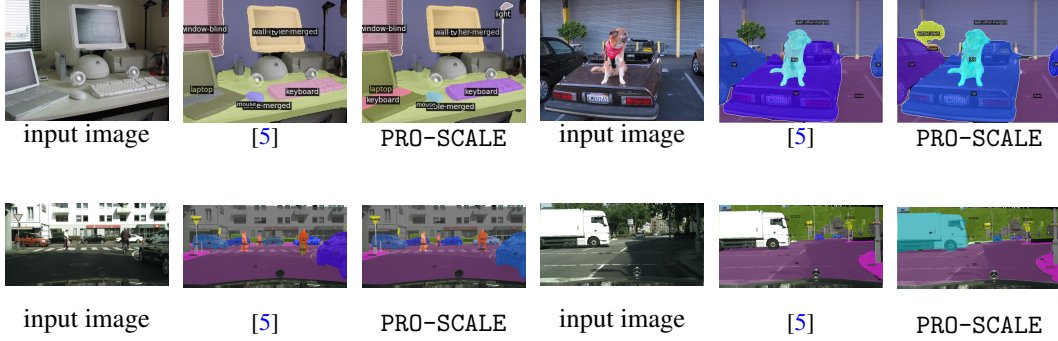


Figure 9: **Qualitative visualizations.** We visualize few examples of predicted panoptic maps from M2F [5] and PRO-SCALE. Even with 52% encoder GFLOPs reduction, PRO-SCALE shows better quality panoptic maps (backbone = SWIN-T, PRO-SCALE config. = (3, 3, 3)). *Zoom-in for best view.*

Variations in encoder configuration. Here, we analyze the impact of PRO-SCALE configuration on model performance in Tab. 7. We can make some key observations. *First*, we observe that PRO-SCALE shows stronger performance if any $p_i > 1$. This is trivial as more computations are allowed for the corresponding layers. *Second*, increasing p_3 and p_2 have different performance-efficiency trade-off: for COCO, p_2 vs. $(p_2 + 3)$ results in only increment of ~ 6.5 GFLOPs with $\sim 1.0\%$ PQ improvement whereas p_3 vs. $(p_3 + 3)$ results in a higher computational load of ~ 32 GFLOPs increase with $\sim 1.6\%$ PQ performance improvement. We make similar observations for the Cityscapes dataset for $(p_1 + 2)$ vs. $(p_2 + 2)$.

Variations in backbone architectures. We analyze the performance of PRO-SCALE with different backbones in Tab. 6. Specifically, we observe the impacts of SWIN-T, Res50, and MViT-T in the segmentation performance. PRO-SCALE is versatile in providing strong performance-efficiency across diverse backbone types.

Variations in backbone pre-trained weights. We analyze the performance of PRO-SCALE with different pre-training strategies of the backbones in Fig. 8. Specifically, we initialize SWIN-T with *supervised learning* (SL) and *self-supervised learning* (SSL) based ImageNet-1K weights. For SSL pre-training, we employ MoBY [36]. We can see that PRO-SCALE can gain performance robustness of SSL weights while providing the same trade-offs as SL weights. For example, when $c_1 = (p_1, p_2, p_3) = (1, 1, 1)$, MoBY shows an improvement of $\sim 1.6\%$ AP_p with the same efficiency gains. On average, MoBY pre-trained backbone provides lower performance degradation compared to SL weights, especially in instance segmentation (Fig. 8, right).

Qualitative analysis. We show some examples of predicted panoptic maps in Fig. 9 with SWIN-T backbone. We set PRO-SCALE configuration to (3, 3, 3). Compared to M2F [5], PRO-SCALE consistently shows strong performance with drastically fewer GLOPs in everyday scenes (*top row of Fig. 9 on COCO*) as well as complex driving scenes (*bottom row of Fig. 9 on Cityscapes*).

5 Conclusion

In this paper, we propose an efficient transformer encoder PRO-SCALE for Mask2Former-style universal segmentation framework. It reduces the computational load by a large margin with minimal degradation in performance. The core principle of PRO-SCALE is to progressively ‘expand’ the length of the tokens with the layers of the encoder. Since we skip using tokens from large scale features in the initial layers of PRO-SCALE, we further employ a token re-calibration module to leverage its benefits for performance improvement without having its computational overhead. Similarly, a light per-pixel embedding module to alleviate the computational overhead arising from creating per-pixel embeddings without much sacrifice in performance. Our extensive experiments demonstrate that PRO-SCALE is significantly lighter than prior prominent methods while maintaining competitive universal segmentation performance.

Supplementary Material for “Progressive Token Length Scaling in Transformer Encoders for Efficient Universal Segmentation”

Abhishek Aich[†], Yumin Suh[†], Samuel Schuster[†], Manmohan Chandraker^{†,‡}
[†]NEC Laboratories, America, USA, [‡]University of California, San Diego, USA

Contents

A Experiment Details	10
Datasets.	10
Baselines.	10
Training details.	11
Loss functions.	11
B Additional Results	11
Object detection.	11
Open-vocab universal segmentation.	11
LPE pooling analysis.	12
Token redundancy visualization.	12
TRC effect visualization.	12
Larger backbone analysis.	12

List of Figures

F1	Token redundancy visualization	11
F2	Effect of TRC module	12

List of Tables

T1	PRO-SCALE for object detection	11
T2	PRO-SCALE for open-vocabulary segmentation	11
T3	LPE pooling analysis	11
T4	Impact of large backbones.	13

A Experiment Details

Datasets. We examine PRO-SCALE with two image segmentation datasets: COCO [21] (80 “things”, 53 “stuff” categories) and Cityscapes [32] (8 “things”, 11 “stuff” categories). COCO has 118K training and 5K validation images. Cityscapes has 2975 training and 500 validation images.

Baselines. We compare our proposed framework with the original M2F, along with some recently proposed efficient transformer encoders for detection [8, 18, 19]. Specifically, we replace the transformer encoder of M2F with encoder architectures proposed in Lite-DETR [18] and RT-DETR [19]. We call these Lite-M2F and RT-M2F, respectively. Note that, we opted for the “Lite-DETR H3L1-(6+1)×1” setup without its key-aware deformable attention [18]. However, we modified this setup to (5+1) when implementing Lite-M2F. For completeness, we also compare with recent non-M2F-style panoptic segmentation models YOSO [13], RAP-SAM [30] and ReMax [15].

Table T1: **PRO-SCALE for object detection.** PRO-SCALE can easily work with DETR [11] based object detection models (here, DINO [24]) and reduce the computations while having better performance. The PRO-SCALE configuration is $(p_1, p_2, p_3, p_4) = (3, 3, 3, 3)$, backbone is Res50, training dataset is COCO, and trained for 12 epochs.

Model	Performance		GFLOPs (% decrement)
	AP	AP50	Encoder
DINO [24]	49.0	66.60	179.00
+ PRO-SCALE	49.4	66.67	126.00 (-29.61)

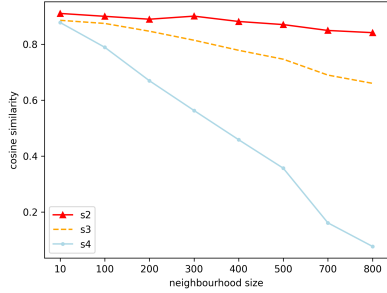


Figure F1: **Token redundancy visualization.**

Table T2: **PRO-SCALE for open-vocabulary segmentation.** PRO-SCALE can easily work with M2F based open-vocab universal segmentation [42] and reduce the computations while having better performance. The PRO-SCALE configuration is $(p_1, p_2, p_3) = (3, 3, 3)$, backbone is Res50, and training dataset is COCO.

Model	Performance(↑)		GFLOPs (↓)
	COCO	ADE20K	Total
MaskCLIP [42]	29.98	15.12	552.8
+ PRO-SCALE	34.53	16.53	489.8

Table T3: **LPE pooling analysis.** We observe that max-pooling provides better results with PRO-SCALE than average pooling. The PRO-SCALE configuration is $(p_1, p_2, p_3) = (3, 3, 3)$, backbone is Res50, training dataset is Cityscapes.

Pooling	PQ (↑)
avg-pooling	61.47
max-pooling	61.87

Training details. All our training details and underlying strategy follow [5], including for our baselines. We use Detectron2 [38] and PyTorch [39] for implementation. We employ the AdamW optimizer [40] with a step learning rate schedule. The initial learning rate is 0.0001. The backbone learning rate is multiplied with 0.1 and its weight decay is set as 0.05. We decay the learning rate at 0.9 and 0.95 fractions of the total training steps by a factor of 10. For COCO, our models are trained for 50 epochs. For Cityscapes, we use 90k iterations. Batch size is set as 16. For data augmentation and calculating GFLOPs, we follow the strategies exactly as M2F. We report the average GFLOPs for all cases. We use distributed training with 8 A6000 GPUs.

Loss functions. We use the exact same loss functions and weights as [5]. In particular, we use the binary cross-entropy loss and the dice loss [41] for our mask loss. Both loss functions use a weight of 5.0. The final loss is a combination of mask loss and classification loss (cross-entropy loss). We set the classification loss weight as 2.0 for all classes, except 0.1 for the ‘no object’ class. Finally, we apply the identical post-processing methodology as described in [5] to obtain the desired output formats for panoptic, semantic, and instance segmentation predictions.

B Additional Results

Object detection. We applied PRO-SCALE to object detection on DINO [24]. Clearly, PRO-SCALE can integrate with object detection models and improve their accuracy and efficiency trade-off. All the models are trained with COCO dataset. The PRO-SCALE configuration is $(p_1, p_2, p_3) = (3, 3, 3)$. The backbone is Res50.

Open-vocab universal segmentation. We used a recent state-of-the-art open-vocabulary image segmentation method MaskCLIP [42]. Our method PRO-SCALE can easily work with M2F based open-vocab segmentation and reduce the computations while having better performance. In the table below, we followed training and testing protocols of [42] and trained our model with COCO train set. We perform evaluation on COCO val set and cross-evaluation on ADE20K [43] val set. The PRO-SCALE configuration is $(p_1, p_2, p_3) = (3, 3, 3)$ and the backbone is Res50. Note that we can employ a different PRO-SCALE configuration to further reduce the computations.

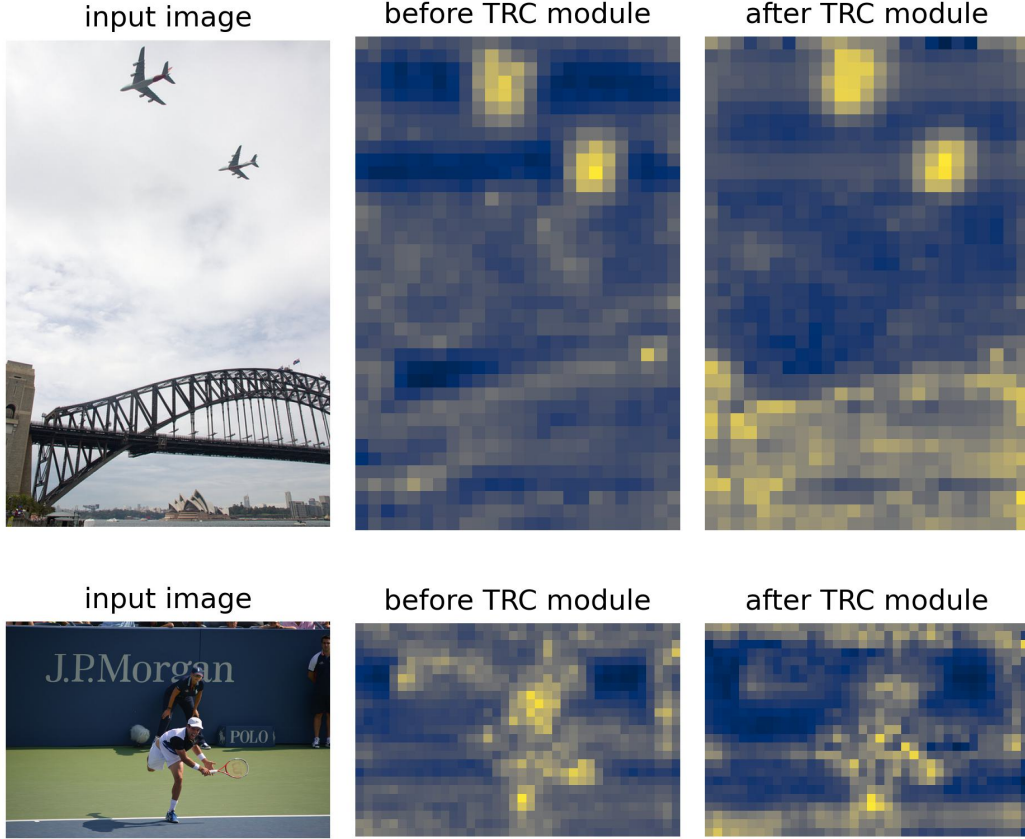


Figure F2: **Effect of TRC module.** It can be observed that the TRC module introduces stronger focus on parts of images that need to be segmented by the model.

LPE pooling analysis. We analyzed the LPE module with ‘average pooling’ in place of ‘max-pooling’ on the Cityscapes dataset with Res50 backbone and $(p_1, p_2, p_3) = (3, 3, 3)$. We observed that the performance of the LPE module performs better with max-pooling (61.87% PQ) than average pooling (61.47% PQ).

Token redundancy visualization. We provide an explicit qualitative visualization that proves the token redundancy in early stages of the transformer encoder in Fig. F1. This analysis is on 100 randomly chosen images from COCO val set. In this figure, the x -axis represents the distance of neighborhood tokens from the candidate token (along the token dimension) and the y -axis represents the (average across the number of images) cosine similarity between the two. It can be observed that in larger scale tokens, the token similarity is higher than smaller token as the neighborhood distance increases. This clearly suggests that the information redundancy of larger scale tokens is comparatively higher than smaller scale tokens.

TRC effect visualization. We provide visualizations of impact of our token re-calibration (TRC) module in two examples shown in Fig. F2. It can be observed that the TRC module introduces stronger focus on parts of images that need to be segmented by the model.

Larger backbone analysis. We present some additional results with larger backbones namely ResNet101, SWIN-Small, SWIN-Base, and SWIN-Large on Cityscapes dataset in Fig. T4. PRO-SCALE reduces GFLOPs in all cases while providing a strong accuracy-efficiency trade-off. The PRO-SCALE configuration is $(p_1, p_2, p_3) = (3, 3, 3)$. Note that, we can also employ a different PRO-SCALE configuration (p_1, p_2, p_3) to further reduce the computations.

Table T4: **Impact of large backbones.** PRO-SCALE can provide significant efficiency boosts across various backbones. Here, $(p_1, p_2, p_3) = (3, 3, 3)$, dataset = Cityscapes.

Backbone type	Performance (\uparrow)			GFLOPs (\downarrow), (% decrement)	
	PQ	mIOU _p	AP _p	Total	Tx. Enc.
SWIN-S	64.80	81.80	40.70	724.3	281
	64.41	80.19	39.90	578.5 (-20.13)	135 (-51.96)
SWIN-B	66.10	82.70	42.80	1051.2	283
	65.27	81.97	41.12	905.4 (-13.87)	137 (-51.59)
SWIN-L	66.60	82.90	43.60	1949.7	287
	65.93	82.77	41.80	1803.9 (-7.48)	141 (-50.87)
Res101	62.40	78.60	37.70	679.7	291
	61.28	76.50	36.49	533.9 (-21.45)	145 (-50.17)

References

- [1] Kaiming He, Georgia Gkioxari, Piotr Dollár, and Ross Girshick. Mask r-cnn. In *Proceedings of the IEEE international conference on computer vision*, pages 2961–2969, 2017.
- [2] Zhuowen Tu. Auto-context and its application to high-level vision tasks. In *2008 IEEE Conference on Computer Vision and Pattern Recognition*, pages 1–8. IEEE, 2008.
- [3] Alexander Kirillov, Kaiming He, Ross Girshick, Carsten Rother, and Piotr Dollár. Panoptic segmentation. In *Proceedings of the IEEE/CVF conference on computer vision and pattern recognition*, pages 9404–9413, 2019.
- [4] Bowen Cheng, Alex Schwing, and Alexander Kirillov. Per-pixel classification is not all you need for semantic segmentation. *Advances in Neural Information Processing Systems*, 34: 17864–17875, 2021.
- [5] Bowen Cheng, Ishan Misra, Alexander G. Schwing, Alexander Kirillov, and Rohit Girdhar. Masked-attention mask transformer for universal image segmentation. In *CVPR*, 2022.
- [6] Jitesh Jain, Jiachen Li, Mang Tik Chiu, Ali Hassani, Nikita Orlov, and Humphrey Shi. Oneformer: One transformer to rule universal image segmentation. In *Proceedings of the IEEE/CVF Conference on Computer Vision and Pattern Recognition*, pages 2989–2998, 2023.
- [7] Xiuye Gu, Yin Cui, Jonathan Huang, Abdullah Rashwan, Xuan Yang, Xingyi Zhou, Golnaz Ghiasi, Weicheng Kuo, Huizhong Chen, Liang-Chieh Chen, et al. Dataseg: Taming a universal multi-dataset multi-task segmentation model. *Advances in Neural Information Processing Systems*, 36, 2024.
- [8] Niccolò Cavagnero, Gabriele Rosi, Claudia Cuttano, Francesca Pistilli, Marco Ciccone, Giuseppe Averta, and Fabio Cermelli. Pem: Prototype-based efficient maskformer for image segmentation. *arXiv preprint arXiv:2402.19422*, 2024.
- [9] Gabriele Rosi, Claudia Cuttano, Niccolò Cavagnero, Giuseppe Averta, and Fabio Cermelli. The revenge of bisenet: Efficient multi-task image segmentation. *arXiv preprint arXiv:2404.09570*, 2024.
- [10] Ashish Vaswani, Noam Shazeer, Niki Parmar, Jakob Uszkoreit, Llion Jones, Aidan N Gomez, Łukasz Kaiser, and Illia Polosukhin. Attention is all you need. *Advances in neural information processing systems*, 30, 2017.
- [11] Nicolas Carion, Francisco Massa, Gabriel Synnaeve, Nicolas Usunier, Alexander Kirillov, and Sergey Zagoruyko. End-to-end object detection with transformers. In *European conference on computer vision*, pages 213–229. Springer, 2020.

- [12] Abdullah Rashwan, Jiageng Zhang, Ali Taalimi, Fan Yang, Xingyi Zhou, Chaochao Yan, Liang-Chieh Chen, and Yeqing Li. Maskconver: Revisiting pure convolution model for panoptic segmentation. In *Proceedings of the IEEE/CVF Winter Conference on Applications of Computer Vision*, pages 851–861, 2024.
- [13] Jie Hu, Linyan Huang, Tianhe Ren, Shengchuan Zhang, Rongrong Ji, and Liujuan Cao. You only segment once: Towards real-time panoptic segmentation. In *Proceedings of the IEEE/CVF Conference on Computer Vision and Pattern Recognition*, pages 17819–17829, 2023.
- [14] Abdallah Ammar, Mahmoud I. Khalil, and Cherif Salama. Rt-yoso: Revisiting yoso for real-time panoptic segmentation. In *2023 5th Novel Intelligent and Leading Emerging Sciences Conference (NILES)*, pages 306–311, 2023. doi: 10.1109/NILES59815.2023.10296714.
- [15] Shuyang Sun, Weijun Wang, Qihang Yu, Andrew Howard, Philip Torr, and Liang-Chieh Chen. Remax: Relaxing for better training on efficient panoptic segmentation. *arXiv preprint arXiv:2306.17319*, 2023.
- [16] Kaiming He, Xiangyu Zhang, Shaoqing Ren, and Jian Sun. Deep residual learning for image recognition. In *Proceedings of the IEEE conference on computer vision and pattern recognition*, pages 770–778, 2016.
- [17] Ze Liu, Yutong Lin, Yue Cao, Han Hu, Yixuan Wei, Zheng Zhang, Stephen Lin, and Baining Guo. Swin transformer: Hierarchical vision transformer using shifted windows. In *Proceedings of the IEEE/CVF international conference on computer vision*, pages 10012–10022, 2021.
- [18] Feng Li, Ailing Zeng, Shilong Liu, Hao Zhang, Hongyang Li, Lei Zhang, and Lionel M Ni. Lite detr: An interleaved multi-scale encoder for efficient detr. In *Proceedings of the IEEE/CVF Conference on Computer Vision and Pattern Recognition*, pages 18558–18567, 2023.
- [19] Wenyu Lv, Shangliang Xu, Yian Zhao, Guanzhong Wang, Jinman Wei, Cheng Cui, Yuning Du, Qingqing Dang, and Yi Liu. Dets beat yolos on real-time object detection. *arXiv preprint arXiv:2304.08069*, 2023.
- [20] Zhuyu Yao, Jiangbo Ai, Boxun Li, and Chi Zhang. Efficient detr: improving end-to-end object detector with dense prior. *arXiv preprint arXiv:2104.01318*, 2021.
- [21] Tsung-Yi Lin, Michael Maire, Serge Belongie, James Hays, Pietro Perona, Deva Ramanan, Piotr Dollár, and C Lawrence Zitnick. Microsoft coco: Common objects in context. In *Computer Vision—ECCV 2014: 13th European Conference, Zurich, Switzerland, September 6-12, 2014, Proceedings, Part V 13*, pages 740–755. Springer, 2014.
- [22] Feng Li, Hao Zhang, Huaizhe Xu, Shilong Liu, Lei Zhang, Lionel M Ni, and Heung-Yeung Shum. Mask DINO: Towards a unified transformer-based framework for object detection and segmentation. In *Proceedings of the IEEE/CVF Conference on Computer Vision and Pattern Recognition*, pages 3041–3050, 2023.
- [23] Zheng Ding, Jieke Wang, and Zhuowen Tu. Open-vocabulary panoptic segmentation with maskclip. *arXiv preprint arXiv:2208.08984*, 2022.
- [24] H Zhang, F Li, S Liu, L Zhang, H Su, J Zhu, LM Ni, and HY Shum. Dino: Detr with improved denoising anchor boxes for end-to-end object detection. arxiv 2022. *arXiv preprint arXiv:2203.03605*, 2022.
- [25] Jingdong Wang, Ke Sun, Tianheng Cheng, Borui Jiang, Chaorui Deng, Yang Zhao, Dong Liu, Yadong Mu, Mingkui Tan, Xinggang Wang, Wenyu Liu, and Bin Xiao. Deep high-resolution representation learning for visual recognition. *TPAMI*, 2019.
- [26] Daan de Geus, Panagiotis Meletis, and Gijs Dubbelman. Fast panoptic segmentation network. *IEEE Robotics and Automation Letters*, 5(2):1742–1749, 2020.
- [27] Weixiang Hong, Qingpei Guo, Wei Zhang, Jingdong Chen, and Wei Chu. Lpsnet: A lightweight solution for fast panoptic segmentation. In *Proceedings of the IEEE/CVF Conference on Computer Vision and Pattern Recognition*, pages 16746–16754, 2021.

- [28] Rui Hou, Jie Li, Arjun Bhargava, Allan Raventos, Vitor Guizilini, Chao Fang, Jerome Lynch, and Adrien Gaidon. Real-time panoptic segmentation from dense detections. In *Proceedings of the IEEE/CVF Conference on Computer Vision and Pattern Recognition*, pages 8523–8532, 2020.
- [29] Josip Šarić, Marin Oršić, and Siniša Šegvić. Panoptic swiftnet: Pyramidal fusion for real-time panoptic segmentation. *Remote Sensing*, 15(8):1968, 2023.
- [30] Shilin Xu, Haobo Yuan, Qingyu Shi, Lu Qi, Jingbo Wang, Yibo Yang, Yining Li, Kai Chen, Yunhai Tong, Bernard Ghanem, et al. Rap-sam: Towards real-time all-purpose segment anything. *arXiv preprint arXiv:2401.10228*, 2024.
- [31] Xizhou Zhu, Weijie Su, Lewei Lu, Bin Li, Xiaogang Wang, and Jifeng Dai. Deformable detr: Deformable transformers for end-to-end object detection. *arXiv preprint arXiv:2010.04159*, 2020.
- [32] Marius Cordts, Mohamed Omran, Sebastian Ramos, Timo Rehfeld, Markus Enzweiler, Rodrigo Benenson, Uwe Franke, Stefan Roth, and Bernt Schiele. The cityscapes dataset for semantic urban scene understanding. In *Proceedings of the IEEE conference on computer vision and pattern recognition*, pages 3213–3223, 2016.
- [33] Mark Everingham, SM Ali Eslami, Luc Van Gool, Christopher KI Williams, John Winn, and Andrew Zisserman. The pascal visual object classes challenge: A retrospective. *International journal of computer vision*, 111:98–136, 2015.
- [34] Yanghao Li, Chao-Yuan Wu, Haoqi Fan, Kartikeya Mangalam, Bo Xiong, Jitendra Malik, and Christoph Feichtenhofer. Mvitv2: Improved multiscale vision transformers for classification and detection. In *CVPR*, 2022.
- [35] Jia Deng, Wei Dong, Richard Socher, Li-Jia Li, Kai Li, and Li Fei-Fei. Imagenet: A large-scale hierarchical image database. In *2009 IEEE conference on computer vision and pattern recognition*, pages 248–255. Ieee, 2009.
- [36] Zhenda Xie, Yutong Lin, Zhuliang Yao, Zheng Zhang, Qi Dai, Yue Cao, and Han Hu. Self-supervised learning with swin transformers. *arXiv preprint arXiv:2105.04553*, 2021.
- [37] Olga Russakovsky, Jia Deng, Hao Su, Jonathan Krause, Sanjeev Satheesh, Sean Ma, Zhiheng Huang, Andrej Karpathy, Aditya Khosla, Michael Bernstein, et al. Imagenet large scale visual recognition challenge. *International journal of computer vision*, 115:211–252, 2015.
- [38] Yuxin Wu, Alexander Kirillov, Francisco Massa, Wan-Yen Lo, and Ross Girshick. Detectron2. <https://github.com/facebookresearch/detectron2>, 2019.
- [39] Adam Paszke, Sam Gross, Francisco Massa, Adam Lerer, James Bradbury, Gregory Chanan, Trevor Killeen, Zeming Lin, Natalia Gimelshein, Luca Antiga, et al. Pytorch: An imperative style, high-performance deep learning library. *Advances in neural information processing systems*, 32, 2019.
- [40] Ilya Loshchilov and Frank Hutter. Decoupled weight decay regularization. *arXiv preprint arXiv:1711.05101*, 2017.
- [41] Fausto Milletari, Nassir Navab, and Seyed-Ahmad Ahmadi. V-net: Fully convolutional neural networks for volumetric medical image segmentation. In *2016 fourth international conference on 3D vision (3DV)*, pages 565–571. Ieee, 2016.
- [42] Zhuowen Tu Zheng Ding, Jieke Wang. Open-vocabulary universal image segmentation with maskclip. In *International Conference on Machine Learning*, 2023.
- [43] Bolei Zhou, Hang Zhao, Xavier Puig, Sanja Fidler, Adela Barriuso, and Antonio Torralba. Scene parsing through ade20k dataset. In *Proceedings of the IEEE conference on computer vision and pattern recognition*, pages 633–641, 2017.